RSC Advances

This is an *Accepted Manuscript*, which has been through the Royal Society of Chemistry peer review process and has been accepted for publication.

Accepted Manuscripts are published online shortly after acceptance, before technical editing, formatting and proof reading. Using this free service, authors can make their results available to the community, in citable form, before we publish the edited article. This *Accepted Manuscript* will be replaced by the edited, formatted and paginated article as soon as this is available.

You can find more information about *Accepted Manuscripts* in the Information for Authors.

Please note that technical editing may introduce minor changes to the text and/or graphics, which may alter content. The journal's standard Terms & Conditions and the Ethical guidelines still apply. In no event shall the Royal Society of Chemistry be held responsible for any errors or omissions in this *Accepted Manuscript* or any consequences arising from the use of any information it contains.

ROYAL SOCIETY OF CHEMISTRY

www.rsc.org/advances

A quinoline based Schiff-base compound as pH sensor†

Shibashis Halder, Sudipto Dey and Partha Roy*

Department of Chemistry, Jadavpur University, Jadavpur, Kolkata-700 032, India
E-mail: proy@chemistry.jdvu.ac.in; Tel: +91-3324572267; Fax: +91-3324146414
†Electronic supplementary information (ESI) available. For ESI format see DOI .....

Abstract

A new Schiff-base compound, 1,4-bis-(quinolin-6-ylimino methyl)benzene **(BQB)**, has been synthesized by the reaction between terephthaldehyde and 6-aminoquinoline (1:2 ratio) and characterized by elemental analysis and different spectroscopic methods. The Schiff-base compound, designated as **BQB**, undergoes protonation in acidic medium and has been designated as **PBQB**. **PBQB** shows emission intensity at 550 nm at low pH and with the increase in pH, the intensity of the peak at 550 nm decreases with simultaneous shift of the emission band to 453 nm. The intensity of the peak at 453 nm increases as pH of the medium is raised and the phenomenon is found to be reversible. Reversibility of fluorescence intensity of **BQB** with pH shows that the system is stable in both basic and acidic media. Absorption spectrum of the compound shows band at 380 nm with a strong shoulder at 402 nm in low pH which changes to 344 nm at higher pH region. Naked eye detection of colour change at different pH regions is possible using the probe. Position of absorption band of **BQB** is changed in acidic medium due to protonation of the ring nitrogen atom present in it as reflected by theoretical studies. We have applied our probe to detect the pH region of river water.

RSC Advances Accepted Manuscript

Introduction

Hydrogen or hydroxyl ion is one of the most available small molecules/ions present in physiological, biological and chemical systems. The presence of H^+ or OH^- in aqueous media is typically evaluated based on its pH value. pH is one of the most important factors for wide range of applications in the field of chemical syntheses, medicine, environmental science, life sciences, industry, sewage purification scheme, *etc*.[1] Many methods are in practice for the measurement of pH, for example, microelectrodes, absorption spectroscopy, nuclear magnetic resonance spectroscopy, fluorescence spectroscopy, *etc*.[2] Among these, fluorescence spectroscopy has become particularly promising because of its simple operation, ease of application, noninvasiveness, high selectivity, low cost and real-time visualization.[3] However, in laboratories, still today pH of a medium is mostly determined by using instruments based on glass electrode. But, fluorescent sensors have many advantages over the traditional glass pH electrodes which have several restrictions *e.g*. electrical interference, presence of acid error and possible damage.[4] Thus, remarkable research efforts have been directed over the last few decades to the measurement of pH accurately[5] and a huge thrust has been given on the development of fluorescent pH sensors. pH sensors so far reported are mainly based on xanthenes, BODIPY, cyanine and other fluorochromes,[5] acrylamide,[6] rhodamine,[7] hybrid of fluorescein/cyanine,[8] optical fibre,[9] rhodamine–napthalimide conjugate,[10] *etc*. pH sensors which were developed based on common pH-sensitive indicator dyes *e.g*. fluorescein, pyrene, xanthenes, *etc*. suffer some limitations. There are questions about the brightness, photostability of probe and solubility in water. These compounds have relatively short excitation wavelength which results in autofluorescence. For these reasons, researchers are actively engaged in developing different pH indicators which are devoid of the related limitations.

We report here synthesis, characterization and exploration of pH sensing behavior of 1,4-bis-(quinolin-6-yliminomethyl)benzene (**BQB**) (Scheme 1). It was synthesized by Schiff-base condensation between terephthaldehyde and 6-aminoquinoline (1:2 ratio) and characterized by elemental analysis and various spectroscopic methods. It behaves as a ratiometric fluorescence sensor for pH and is converted to its protonated form (**PBQB**) in acidic region. Emission intensity of **PBQB** at 550 nm decreases whereas emission intensity of **BQB** at 453 nm increases with the increase in pH when the probe is excited at 380 nm. Some theoretical calculations have been performed to get a better look picture of the phenomenon.

RSC Advances Accepted Manuscript

Experimental Section

Materials and Physical methods

Terephthaldehyde and 6-aminoquinoline were purchased from Sigma Aldrich and used without purification. Other reagents were purchased from commercial source and used without further purification. Solvents used for spectroscopic studies were purified and dried by standard procedures before use.[11] Elemental analysis was carried out with a 2400 Series-II CHN analyzer, Perkin Elmer, USA. FT-IR spectra were obtained on a Perkin Elmer spectrometer (Spectrum Two) with the samples by attenuated total reflectance (ATR) technique. Absorption spectra were studied using a Shimadzu UV 2100 spectrophotometer and emission spectra on a Shimadzu RF-5301-PC spectrophotometer. ESI-MS^+ spectra were recorded on a QTOF Micro YA263 mass spectrometer. NMR spectra of the compounds were recorded on Bruker 300 MHz spectrometer.

Fluorescence quantum yields (Φ) of **BQB** at different *p*H were determined by using the formula:

$$\Phi_{sample} = \{(OD_{standard} \times A_{sample} \times \eta^2_{sample})/(OD_{sample} \times A_{standard} \times \eta^2_{standard})\} \times \Phi_{standard}$$

where A is the area under the emission spectral curve, OD is optical density of the compound at the excitation wavelength and η is the refractive index of the solvent, $\Phi_{standard}$ is the quantum yield of standard (quinine sulphate) (Φ = 0.546 in water, λ_{ex} = 350 nm) (Φ = 0.077, 0.1 and 0.12 at pH 6, pH 7 and pH 8 respectively).

Synthesis of 1,4-bis-(quinolin-6-yliminomethyl)benzene (BQB)

Terephthaldehyde (1.34 g, 10 mmol) in 20 mL of methanol was added to a 20 mL of methanolic solution of 6-aminoquinoline (2.88 g, 20 mmol) and stirred for 30 min. The mixture was refluxed for 6 h and was cooled to room temperature when a light golden yellow precipitate was obtained. The mixture was filtered to collect the yellow product and dried. Then it was dissolved in toluene by heating at around 70 °C. This toluene solution was allowed to stay without any disturbance. Light yellow needle shaped crystalline material was obtained after two days. Yield: 2.7g (70%). Anal. Calc. (%) for $C_{26}H_{18}N_4$ (M= 386 g/mol): C, 80.83; H, 4.66; N, 14.51. Found: C, 80.75; H, 4.58; N, 14.44. ESI-MS^+ (*m/z*): 387019 (BQB + H^+); 419.22 (BQB + CH_3OH + H^+); 194.09 (BQB + H^+ + H^+); 210.11 (BQB + CH_3OH + H^+ + H^+). ^{1}H NMR (300 MHz, $CDCl_3$; δ): 7.45 (dd, 1H, J_1 = 4.26 Hz, J_2 = 8.22 Hz, Ar), 7.64 (d, J=2.14 Hz, 1H, Ar), 7.73

RSC Advances Accepted Manuscript

(dd, 1H, J_1 = 2.30 Hz, J_2 = 8.86 Hz, Ar), 8.13-8.23 (overlap, 4H, Ar), 8.70 (s, 1H, imine), 8.93 (dd, 1H, J_1 = 3.14 Hz, J_2 = 5.97 Hz, Ar). ^{13}C NMR (300 MHz, DMSO-d_6; δ): 117.1, 121.6, 124.4, 129.3, 130.0, 130.6, 130.7, 135.9, 138.7, 147.2, 149.7, 149.9 and 160.2.

Theoretical calculations

The ground state (S_0) geometry and lowest lying triplet excited state (T_1) of **BQB** and **PBQB** were fully optimized by DFT/B3LYP method using the Gaussian 03 program.[12] The B3LYP functional has been adopted along with the 6-31G basis set for H, C, N atoms. The absorption and emission spectral properties of **BQB** and **PBQB** in water were calculated by a time-dependent density functional theory (TDDFT)[13] approach associated with the conductor-like polarizable continuum model (CPCM).[14]

Results and Discussion

We designate the Schiff-base compound as **BQB** when it is not protonated and the protonated form as **PBQB**.

PBQB (1×10^{-4} M) exhibits fluorescence emission peak at 550 nm with moderate intensity in pH 2.0 in Britton Robinson Buffer[15] at room temperature when it is excited at 380 nm. Fluorescence intensities of **BQB** have been measured in the pH range of 2.0-11.0 (Fig. 1). With the increase in pH value, intensity of **PBQB** peak at 550 nm decreases gradually and at the same time a new peak at 453 nm starts to emerge. As the pH value increases gradually emission intensity at 453 nm enhances significantly keeping the initial peak at 550 nm as the shoulder. Fluorescence titration experiment of **BQB** *vs.* pH shows an isoemissive point at around 525 nm. Thus, emission intensities at 550 nm and 453 nm are due to **PBQB** and **BQB** respectively. The ratio of fluorescence intensities from the two different forms i.e. **BQB** and **PBQB** (I_{453}/I_{550}) can be determined and plotted against pH values (Fig. 1, inset). From the figure, it is evident that there is almost a linear relationship of the intensity ratio with pH value in the range of 5.0–7.5. The pK_a value of **PBQB** has been determined to be 6.30. The pK_a value has been calculated using the Henderson–Hasselbach type mass action equation: $\log\{(F_{max}–F)/(F–F_{min})\} = pH–pK_a$, where F_{max}, F_{min}, F represent the maximum, minimum and observed fluorescence intensity at a given pH value, respectively (Fig. S6).[16] The value is near to the physiological pH 7.4, indicating that the fluorophore could be an innate pH indicator.

RSC Advances Accepted Manuscript

The stability of Schiff-base compounds in acidic or basic medium may raise a question. A number of Schiff-base compounds have been synthesized using 2-hydroxynapthaldehyde and they have been used as fluorescent sensor for Al^{3+} ion. These Schiff-base compounds show stability towards pH variation.[17] We want **BQB** to suffer pH variation to examine its stability in different pH media. The aqueous solution of the probe exhibits fluorescence reversibility when pH of the solution is adjusted back and forth between pH 4 and pH 10 with 2(M) HCl and 2(M) NaOH solutions. Fig. 2 represents the corresponding array, which indicates that the material has good sensitivity towards pH switched on and off. The change in pH of the medium in the presence of the probe immediately results in alteration of emission intensity of **BQB**. This shows that the pH can be switched to acidic and basic range several times repeatedly without deterioration of on/off character.

Real samples including biological systems are complicated due to the presence of different ions and molecules. To check the effect of different ions including environmentally threatening metal ions and anions, emission intensity of the material was measured at pH 6.5 in the presence of Na^{+}, K^{+}, Zn^{2+}, Mg^{2+}, Cu^{2+}, Mn^{2+}, Fe^{3+}, Co^{2+}, Ca^{2+}, Ni^{2+}, NO_3^{-}, Cl^{-}, SO_4^{2-}, PO_4^{3-} and BO_3^{3-} (Fig. 3). It has been found that the emission intensity is almost unaffected by their presence. Only Cu^{2+}, Mn^{2+} and Fe^{3+} can induce slight decrease in emission intensity of the probe. Similar experiment has been carried out at pH 7.5 to observe effect of some cations and anions on emission intensity of **BQB** at that pH (Fig. S7). It is to mention that there is almost no effect of different ions on the fluorescence intensity of **BQB**. Thus, **BQB** can act reversibly as a fluorescent ratiometric pH sensor in the presence of other relevant ions. Protonation of heterocyclic nitrogen atom[18] enhances the resonance contribution of quinoid forms enabling **BQB** to act as a fluorescent pH sensor.

The UV-visible spectra of **BQB** (1×10^{-4} M) in different pH with Britton Robinson buffer were recorded at room temperature (Fig. 4). **PBQB** shows strong peaks at 380 nm and a strong shoulder at 402 nm in lower pH range. The peak at 380 nm gradually undergoes blue shift with the increase in pH and the intensity at 402 nm decreases with the enhancement of pH. Consequently a new peak appears at 344 nm with the complete disappearance of peak at 380 along with the shoulder. These peaks are due to intraligand charge transfer (see DFT part). The absorbance at longer wavelength is a result of comparatively extended conjugation between quinoline rings and benzene ring.[18] The absorbance value at 344 nm increases with the further

RSC Advances Accepted Manuscript

enhancement in pH of the medium. As a result, an isosbestic point has been noticed at around 363 nm.

It is well known to us that quinoline shows bathochromic shift in acidic medium due to the protonation of heterocyclic nitrogen atom which increases resonance contributions of certain quinoid forms.[19,20] On the other hand, amino group on aromatic ring exhibits strong hypsochromic shift due to addition of proton to the non-heterocyclic nitrogen atom.[19] In the aminoquinolines, tendencies for bathochromic and hypsochromic shifts must exist. A shift of absorption band in acidic solution relative to basic or neutral occurs towards longer wavelengths as in quinoline. It was also reported that in case of acridines that the absorption spectrum shifts towards longer wavelength if the first proton binds with ring nitrogen atom and towards shorter wavelength when first proton goes to nitrogen atom of substituted group. There are two possible binding sites of **BQB** to H^+ ion: the nitrogen atom in the heterocyclic ring and the nitrogen atom in the imine group (the substituted amine group). Thus, H^+ ion is attached to heterocyclic nitrogen atom of **BQB** to convert it to **PBQB** as absorption band of **BQB** at 344 nm shifts to 380 nm on lowering pH of the medium.

Some theoretical calculations were performed to support the observed experimental data of absorption and emission spectra. The ground state (S_0) geometry and lowest lying triplet excited state (T_1) of **BQB** and **PBQB** were fully optimized by DFT/B3LYP method using the Gaussian 03 program.[12] Geometry of optimized structures are shown in Fig. 5. By analyzing the optimized structures we have made some interesting observation. The angle between the two quinoline rings in **BQB** is 56.99° whereas for **PBQB** it is 87.39°. Thus, after protonation, angle between two the quinoline rings in **BQB** has changed by about 30.40° in **PBQB** confirming quite large conformational change (Fig. S9).

On the basis of the optimized ground and excited state geometry structures, the absorption and emission spectral properties of **BQB** and **PBQB** in water were calculated by a time-dependent density functional theory (TD-DFT) approach associated with the conductor-like polarizable continuum model (CPCM). We have computed the lowest 20 singlet–singlet transition and the results of TD calculations were qualitatively very similar. Due to the presence of electronic correlation in the TDDFT (B3LYP) method it can yield more accurate electronic excitation energies. **BQB** and **PBQB** show intense peaks at 330 nm (experimental value: 345 nm) and 385.9 nm, 394 nm (experimental value: 380 nm, 402nm), respectively (Table 1; Fig. 6).

RSC Advances Accepted Manuscript

The electron density at the HOMO of **PBQB** resides at benzene ring but for LUMO + 1 it resides at quinoline rings. In this case, the absorption bands are generally due to intraligand charge transfer transition. The HOMO- LUMO energy gap is lower for the protonated species which explains its higher absorption wavelength (Fig. S10). The calculated electronic density plots for frontier molecular orbitals were prepared by using the GaussView 5 software.

In order to discuss the nature of the emission, we optimize the T_1 states of both species discussed earlier. The most meaningful Frontier Molecular Orbitals of the T_1 state for **BQB** and **PBQB** are listed in Fig. 7 and isodensity surfaces of the Highest and Lowest Singly Occupied Molecular Orbitals, namely HSOMO and LSOMO for those compounds at the relaxed T_1 geometry are shown in Fig. S11. The calculated emission energies, dominant configurations (with larger CI coefficients), transition nature, and the available experimental values are listed in Table 2. The calculated emission wavelengths for **BQB** and **PBQB** also nearly coincides with the experimental value, $\text{Emission}_{\mathbf{BQB}}$ 456.15 nm (experimental value: 453 nm) and $\text{Emission}_{\mathbf{PBQB}}$ 552 nm (experimental value: 559.29 nm).

The Schiff-base compound undergoes a visible color change with the change in pH values in aqueous medium. Photographs in Fig. 8 show color changes of aqueous solution of **BQB** at different pH under visible light and UV light. It can be clearly seen that the color becomes intense yellow as the pH of the solution is lowered to at least 5.0 and with increase in pH, the color fades up gradually and ultimately disappears beyond pH 7. The yellow color of the probe disappears near neutral and basic region. The acidic solution of **BQB**, under ultraviolet radiation, becomes yellow and basic solution of the probe turns bluish white. The color change of **BQB** under visible light and UV-light could be a very practical way to identify different pH regions of a sample.

^{1}H and ^{13}C NMR spectra of **BQB** are given in Fig. S3 and Fig. S4, respectively. ^{1}H NMR spectrum of **BQB** was recorded in DMSO-d_6 in the presence of very minute amount of HCl to assign the possible binding site of H^+ with **BQB** (Fig. S5). The entire aromatic and imine proton peaks shift markedly. However, no peak for NH^+ proton could be detected. So it is not possible to assign surely whether H^+ binds to heterocyclic or azomethine nitrogen atom. But indirectly we can say that it is bound to ring nitrogen atom. There is huge downfield shift in peak position of aromatic proton adjacent to heterocyclic nitrogen atom from 8.93 ppm in **BQB** to 10.11 ppm in **PBQB** (Fig. S3 and S5). It is only possible when H^+ binds to heterocyclic nitrogen atom. Peak

RSC Advances Accepted Manuscript

position for imine proton does change appreciably (8.69 ppm in **BQB** *vs* 8.78 ppm in **PBQB**).This will not be possible if H^+ binds to azomethine nitrogen atom. All other peak positions for aromatic protons change accordingly.

We have applied the probe to monitor acidity/basicity of river water to check whether our system is actually able to detect different pH regions of real system. River basins are, in general, highly populated areas owing to favorable living conditions *e.g.* availability of fertile lands, water for agriculture, industry or drinking purposes, alternative means of transportation, *etc*. Due to human activity, quality of water of a river differs from one region to another. Thus, it is a prerequisite for effective and efficient water management to have reliable information on river water. pH is one of the critical parameters used for the assessment of water quality.[21] pH of drinking water may vary from 6-8.5.[22] River Ganga is one of the prime rivers in India. We have collected water from river Ganga at Patuli, Burdwan district of West Bengal, India (~130 km upstream from Kolkata). pH of the collected water was determined by pH meter to be 7.81. Fluorescence and absorption spectra of the collected river water were measured (Fig. S12 and S13). Fluorescence and absorption spectra of **BQB** in water of Ganga river are quite similar to those of **BQB** in water under similar conditions. We have calculated fluorescence intensities at 453 nm and 550 nm i.e. I_{435}/I_{550} and the corresponding pH of that particular I_{435}/I_{550} value has been evaluated to be 7.88 (Fig. S14). Thus, we have been able to measure pH of river water that is very close to the value of pH of the same water measured by pH meter. We have taken image of this water in the presence of **BQB** under visible and UV light (Fig. 9). It can be clearly seen from the figure that pH region of river water can easily be marked in basic region as water after treatment with **BQB** appears blue under UV irradiation whereas only river water does not show such color. However, under visible light no such distinct difference in color of two samples can be marked. Thus, the Schiff-base compound could be applied to detect pH regions of real sample.

A few of recently published research works on pH sensor are given in Table 3 for comparison of different aspects of the sensors. Our system has some advantages over the others and also it has some disadvantages. **BQB** has been prepared by easy one step synthesis while others are not. **BQB** has comparatively low excitation wavelength. Like many of reported pH sensors, linear response of pH range of our probe is over neutral pH so that acidic and basic region can be detected. Few of the pH sensors measure extreme acid or basic region. The most

RSC Advances Accepted Manuscript

important aspects of our probe are i) simple one step synthesis with commercially available chemicals and ii) ratiometric sensing.

Conclusions

In conclusion, we have been able to synthesize and characterize a new Schiff-base compound (BQB) with a heterocyclic amine. It exhibits ratiometric reversible pH sensing behavior by binding H^+ to the heterocyclic nitrogen atom. Fluorescence, absorption, NMR spectra and theoretical calculations have been carried out to look into the picture of different phenomena. The probe has been applied in real system. It has been used to detect pH region of river water.

Acknowledgements

PR wishes to thank Department of Science and Technology, New Delhi for financial support. SD and SH wish to thank UGC, New Delhi and CSIR, New Delhi, respectively for fellowships. Authors sincerely thank Dr. Tanurima Bhaumik of Department of Chemistry, Jadavpur University for her help regarding NMR spectra analysis.

RSC Advances Accepted Manuscript

References

1 (a) K. Xu and A. M. Klibanov, *J. Am. Chem. Soc*., 1996, **118**, 9815; (b) R. A. Gottlieb and A. Dosanjh, *Proc. Natl. Acad. Sci. U. S. A*., 1996, **93**, 3587.

2 (a) D. Ellis and R.C. Thomas, *Nature* 1976, **262**, 224; (b) R.G. Zhang, S.G. Kelen and J.C. LaManna, *J. Appl. Physiol*. 1990, **68**, 1101; (c) S.J.A. Hesse, G.J.G. Ruijter, C. Dijkema and J. Vissser, *J. Biotechnol*. 2000, **77**, 5.

3 R. Martinez-Manez and F. Sancenon, *Chem. Rev*. 2003, **103**, 4419.

4 G. Mattock and G. R. Taylor, *pH Measurement and Titration*, Heywood, London, 1961, pp. 198–246.

5 X. Li, X. Gao, W. Shi and H. Ma, *Chem. Rev*., 2014, **114**, 590.

6 L. Yin, C. He, C. Huang, W. Zhu, X. Wang, Y. Xu and X. Qian, *Chem. Commun*., 2012, **48**, 4486.

7 (a) H. Zhu, J. Fan, Q. Xu, H. Li, J. Wang, P. Gao and X. Peng, *Chem. Commun*., 2012, **48**, 11766; (b) M. Tian, X. Peng, J. Fan, J. Wang, S. Sun, *Dyes Pigm.*, 2012, **95** 112; (c) Z.-Q. Hua, M. Li, M.-D. Liu, W.-M. Zhuang, G.-K. Li, *Dyes Pigm*., 2013, **96**, 71; (d) D. Aigner, S. M. Borisov, F. J. O. Fernández, J. F. F. Sánchez, R. Saf, I. Klimant, *Talanta*, 2012, 99, 194.

8 Y. Chen, C. Zhu, J. Cen, Y. Bai, W. He and Z. Guo, *Chem. Sci*., 2015, **6**, 3187.

9 (a) C.R. Zamarreño, M. Hernáez, I. Del Villar, I.R. Matías and F.J. Arregui, *Sens. Actuators B*, 2011, **155**, 290; (b) T. H. Nguyen, T. Venugopala, S. Chen, T. Sun, K. T.V. Grattan, S. E. Taylor, P. A. M. Basheer and A. E. Long, *Sens. Actuators B*, 2014, **191**, 498.

10 Q.-J. Maa, H.-P. Li, F. Yang, J. Zhang, X.-F. Wu, Y. Bai and X.-F. Li, *Sens. Actuators B*, 2012, **166– 167**, 68.

11 D. D. Perrin, W. L. F. Armarego, D. R. Perrin, *Purification of Laboratory Chemicals*, Pergamon Press, Oxford, U.K., 1980.

12 M. J. Frisch, et al., Gaussian 03, revision C.02, Gaussian, Inc., Wallingford, CT, 2004.

13 (a) A. D. Becke, *J. Chem. Phys*., 1993, **98**, 5648; (b) P. J. Hay and W. R. Wadt, *J. Chem. Phys*., 1985, **82**, 299; (c) S. Miertus, E. Scrocco and J. Tomasi, *Chem. Phys*., 1981, **55**, 117; (d) V. Barone, M. Cossi and J. Tomasi, *J. Comput. Chem*., 1998, **19**, 404.

14 (a) V. Barone and M. Cossi, *J. Phys. Chem. A*, 1998, **102**, 1995; (b) M. Cossi and V.

RSC Advances Accepted Manuscript

Barone, *J. Chem. Phys*., 2001, **115**, 4708; (c) M. Cossi, N. Rega, G. Scalmani and V. Barone, *J. Comput. Chem*., 2003, **24**, 669.

15 H.T.S. Britton and R. A. Robinson, *J. Chem. Soc*., 1931, 1456.

16 L. Cao, X. Li, S. Wang, S. Li, Y. Li and G. Yang, *Chem. Commun.,* 2014, **50**, 8787.

17 (a) H. Xiao, K.Chen, N. Jiang, D. Cui, G. Yin, J. Wang and R. Wang, *Analyst*, 2014, **139**, 1980; (b) Z. Liu, Y. Li, Y. Ding, Z. Yang, B. Wang, Y. Lic, T. Li, W. Luo, W. Zhu, J. Xie and C. Wang, *Sens. Actuators B*, 2014, **197**, 200; (c) S. Kim, J.Y. Noh, S.J. Park, Y.J. Na, I.H. Hwang, J. Min, C. Kim and J. Kim, *RSC Adv*., 2014, **4**, 18094; (d) S. Dey, S. Halder, A. Mukherjee, K. Ghosh and P. Roy, *Sens. Actuators B*, 2015, **215**, 196.

18 (a) O. Rotthaus, V. Labet, C. Philouze, O. Jarjayes and F. Thomas, *Eur. J. Inorg. Chem.* 2008, 4215; (b) A. Hens, P. Mondal and K. K. Rajak, *Dalton Trans*., 2013, **42**, 14905.

19 E.A. Stech and G.W. Ewing, *J. Am. Chem. Soc*., 1948, **70**, 3397.

20 D.P. Craig and L.N. Short, *J. Chem. Soc*., 1945, 419.

21 M. Rani, P. Akolkar and H.S. Bhamrah, *J. Entomol. Zoo. Studies*, 2013, **1**, 1.

22 A. K. De, *Environmental chemistry (4th edition)*, New age International Publishers, New Delhi, 2002.

23 U. C. Saha, K. Dhara, B. Chattopadhyay, S. K. Mandal, S. Mondal, S. Sen, M. Mukherjee,S. V. Smaalen, P. Chattopadhyay, *Org. Lett.*, 2011, **13**, 4510.

RSC Advances Accepted Manuscript

Table 1: Main calculated optical transition for **BQB** and **PBQB** with Vertical excitation energies (E_{cal}), oscillator strengths (f_{cal}), and type of excitations of the lowest few excited singlets obtained from TDDFT/B3LYP/CPCM method in water

Compound	**Excitation (eV)**	**Electronic transition State**	**excitation (nm)**	**Osc. strength (f)**	**Key transitions**	**Transition assigned**
BQB	3.755	S_0-S_3	330.16	0.2725	(72%) HOMO-2 →LUMO	ILCT
PBQB	3.212	S_0-S_3	385.95	0.0213	(69%) HOMO →LUMO+1	ILCT
	3.151	S_0-S_2	394	0.0802	(65%) HOMO-1 →LUMO	ILCT
				0.0802	(16%) HOMO →LUMO+1	ILCT

Table 2: Calculated triplet excited state of **BQB** and **PBQB** in water based on the lowest lying triplet state (T_1) geometry: main calculated vertical transitions, vertical excitation energies and oscillator strength

Compound	**Excitation (eV)**	**Excited State**	**excitation (nm)**	**Osc. strength (f)**	**Key transitions**	**CI**	**Transition assigned**
BQB	2.718	13	456.15	0.0084	HOMO-1α ← LUMO α	0.43030	ILCT
					HOMO β ← LUMO+1β	0.82583	ILCT
PBQB	2.2168	9	559.29	0.7286	HOMO α ← LUMO+2 α	0.40873	ILCT
					HOMO-5 β ← LUMO β	0.83969	ILCT

RSC Advances Accepted Manuscript

Table 3: Comparison of few aspects of different pH sensors

Structure	Number of steps involved in synthesis	Emission wavelength in nm (Excitation in nm)	pH range (linear response)	pK_a	Ratiometric	Reference
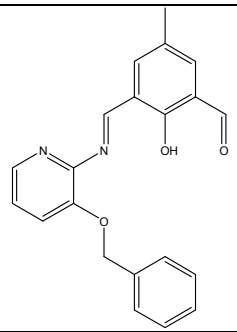	Two	528 (440)	6.0-8.0	6.63	No	23
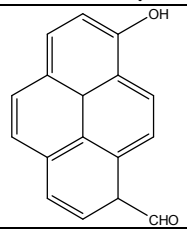	Two	510 and 610 (430)	6.5-8.0	7.8	Yes	16
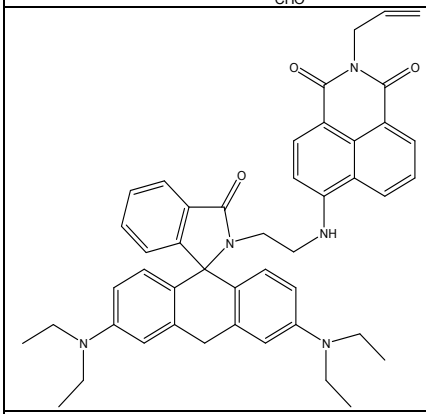	Four	520 (453)	1.0-3.0	2.08	No	10
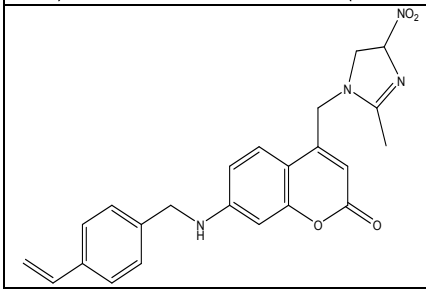	Five	470 (370)	10.5-13.0	11.9	No	9b

RSC Advances Accepted Manuscript

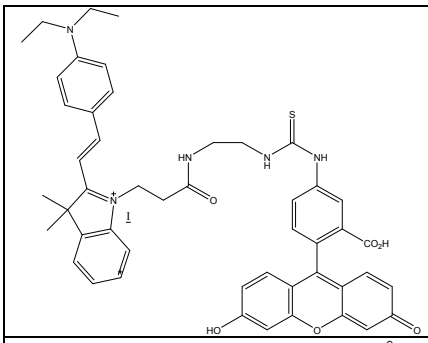	Three	520 (490) & 600 (560)	6.0-8.5	7.33	Yes	8
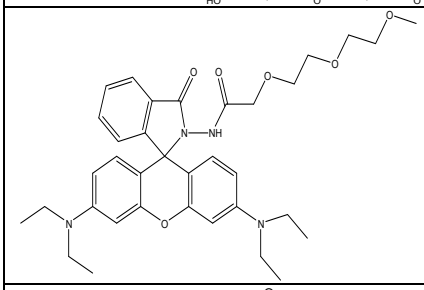	Three	~530 (410)	5.0- 6.5	5.47	No	7a
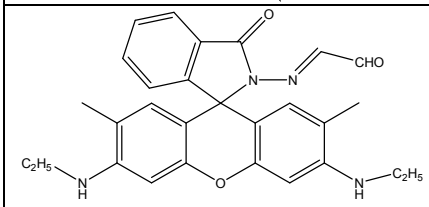	Two	560 (510)	1.5-4.0	2.32	No	7b
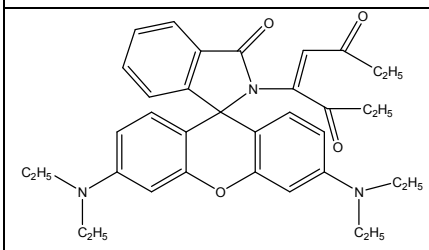	One	585 (500)	4.0-6.5	--	No	7c
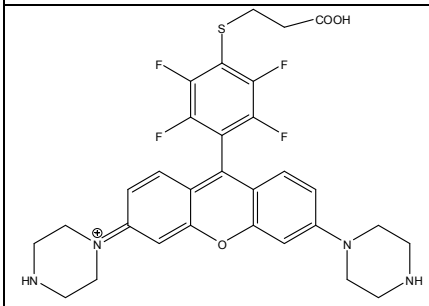	Two	591 (561)	6.5-8.5	--	No	7d
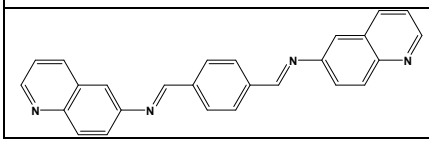	One	453 and 550 (380)	5.0–7.5	6.30	Yes	Present study

RSC Advances Accepted Manuscript

Figure legends:

Scheme S1: Synthesis of **BQB**

Fig. 1: Fluorescence Spectra of the probe (1×10^{-4} M) at pH = 2.0, 2.5, 3.0, 3.5, 4.0, 4.5, 5.0, 5.5, 6.0, 6.5, 7.0, 7.5, 8.0, 8.5, 9.0, 9.5, 10.0, 10.5, 11.0 (λ_{ex} = 380 nm); Inset: Plot of ratio of fluorescence intensities at 453 nm and 550 nm *vs* pH.

Fig. 2: Fluorescence reversibility of **BQB** between pH 4 and pH 10.

Fig. 3: Comparison of fluorescence response of **BQB** at pH 6.5 towards diverse substances at 25 ºC (λ_{ex}: 380 nm); 1, blank; 2, Na^+; 3, K^+; 4, Zn^{2+}; 5, Mg^{2+}; 6, Cu^{2+}; 7, Mn^{2+}; 8, Fe^{3+}; 9, Co^{2+}; 10, Ca^{2+}; 11, Ni^{2+}; 12, NO_3^-; 13, Cl^-; 14, SO_4^{2-}; 15, PO_4^{3-}; 16, BO_3^{3-}.

Fig. 4: Absorption Spectra of **BQB** (1×10^{-4} M) at pH = 2.0, 2.5, 3.0, 3.5, 4.0, 4.5, 5.0, 5.5, 6.0, 6.5, 7.0, 7.5, 8.0, 8.5, 9.0, 9.5, 10.0, 10.5, 11.0.

Fig. 5: Optimized geometries of **BQB** and **PBQB**

Fig. 6: Frontier molecular orbitals involved in the UV-vis absorption

Fig. 7: Frontier molecular orbitals involved in emission of **BQB** and **PBQB** respectively

Fig. 8: **BQB/PBQB** at different pH under UV irradiation (above) and visible light (below)

Fig. 9: Images of water of river Ganga in the presence (left) and in absence (right) of **BQB** under UV irradiation (above) and visible light (below)

RSC Advances Accepted Manuscript

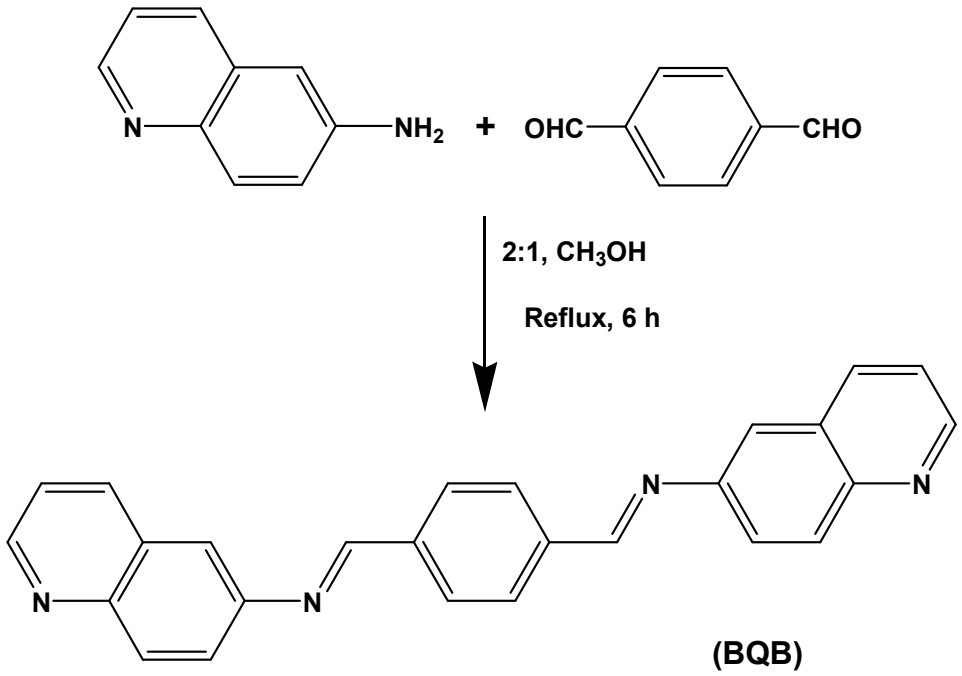

Scheme 1

RSC Advances Accepted Manuscript

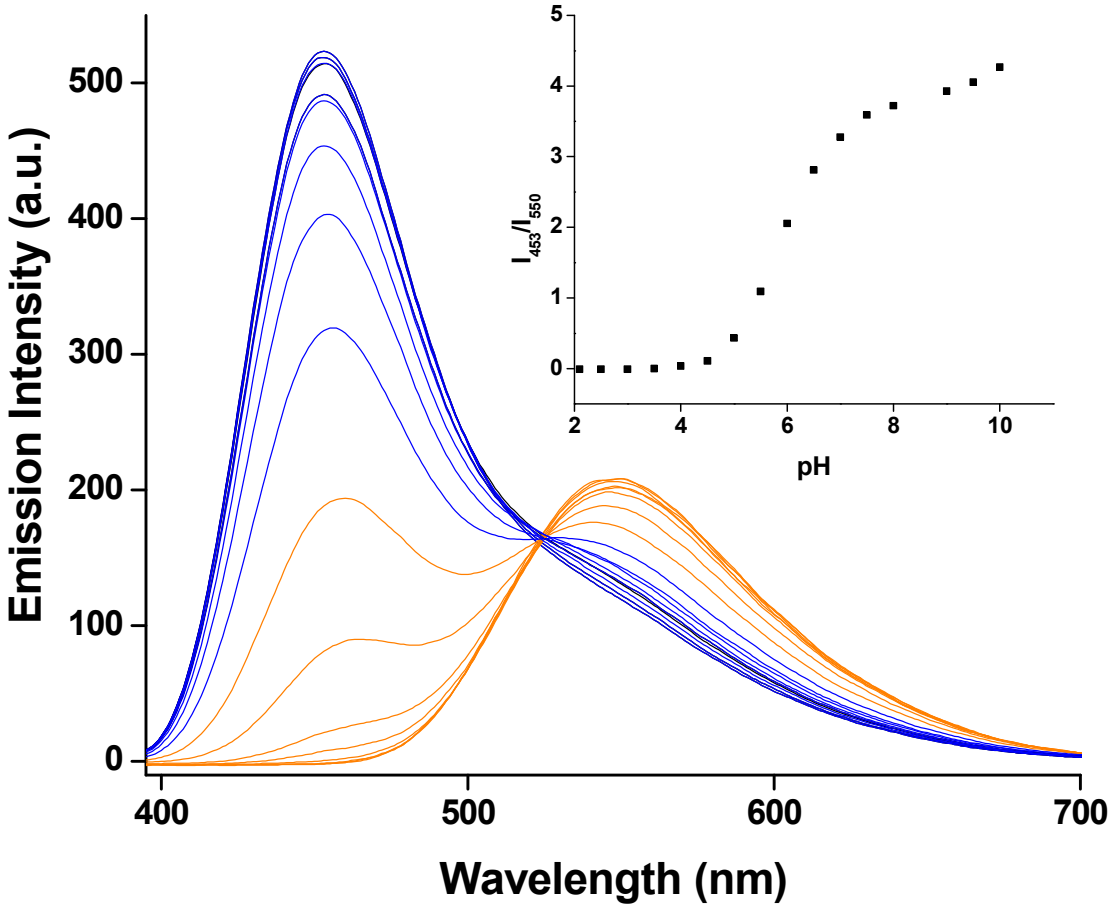

Fig. 1

RSC Advances Accepted Manuscript

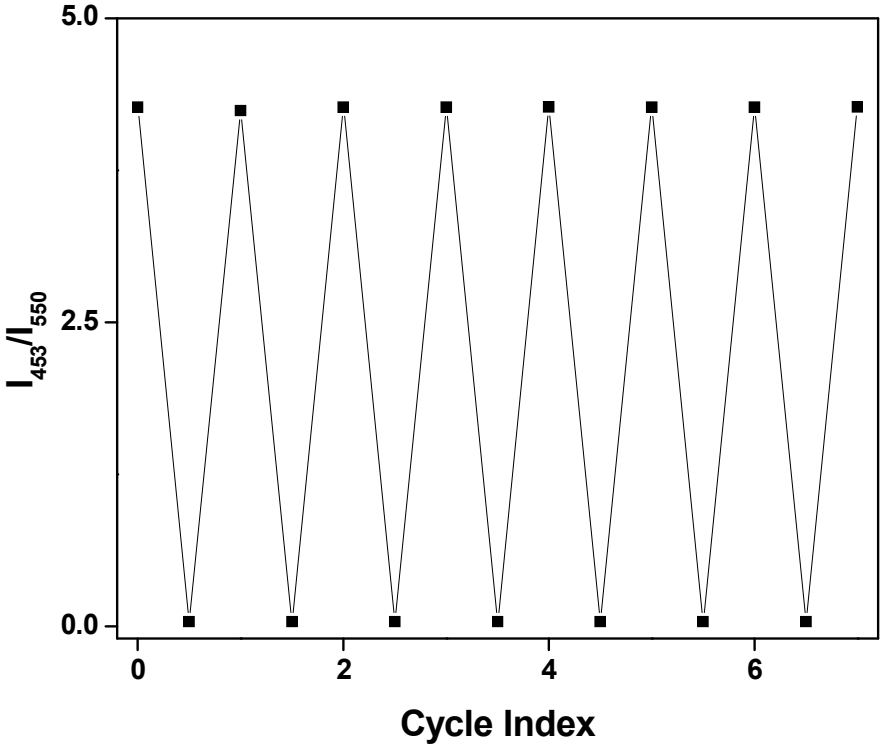

Fig. 2

RSC Advances Accepted Manuscript

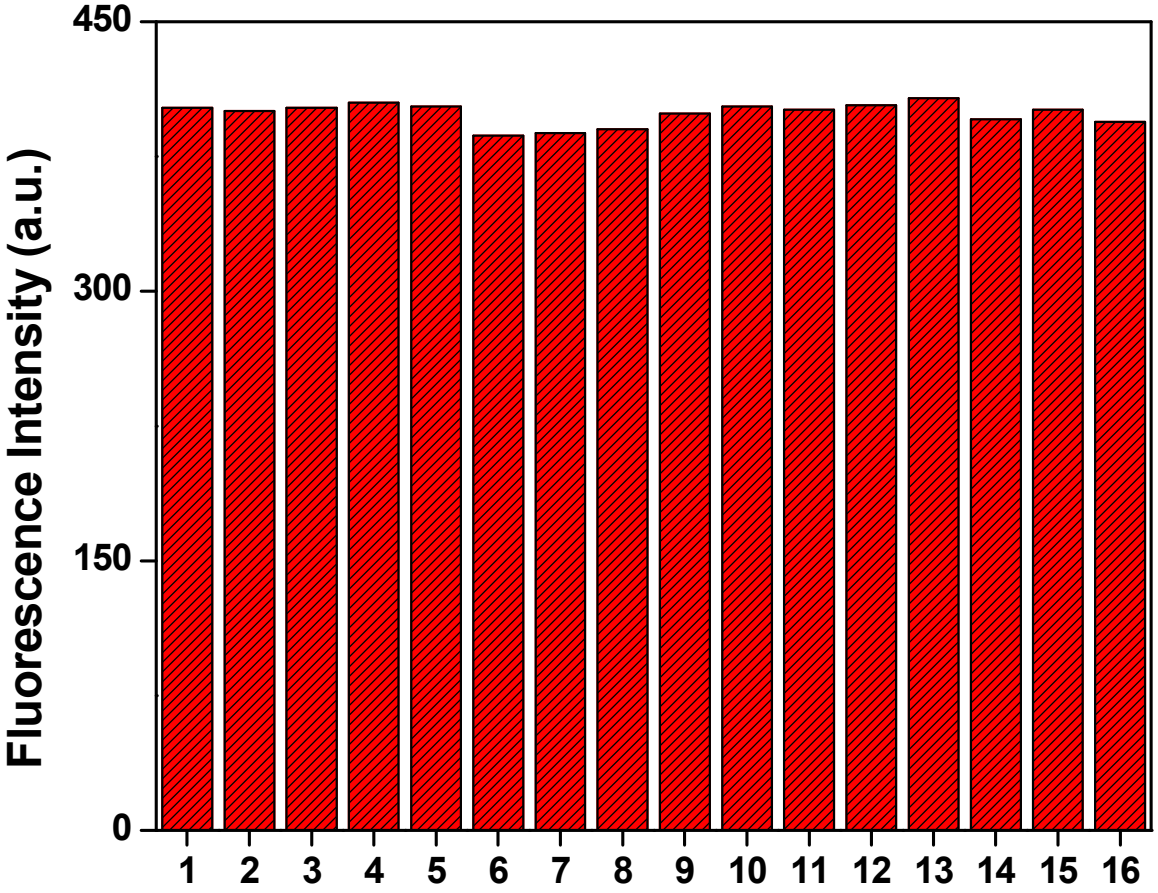

Fig. 3

RSC Advances Accepted Manuscript

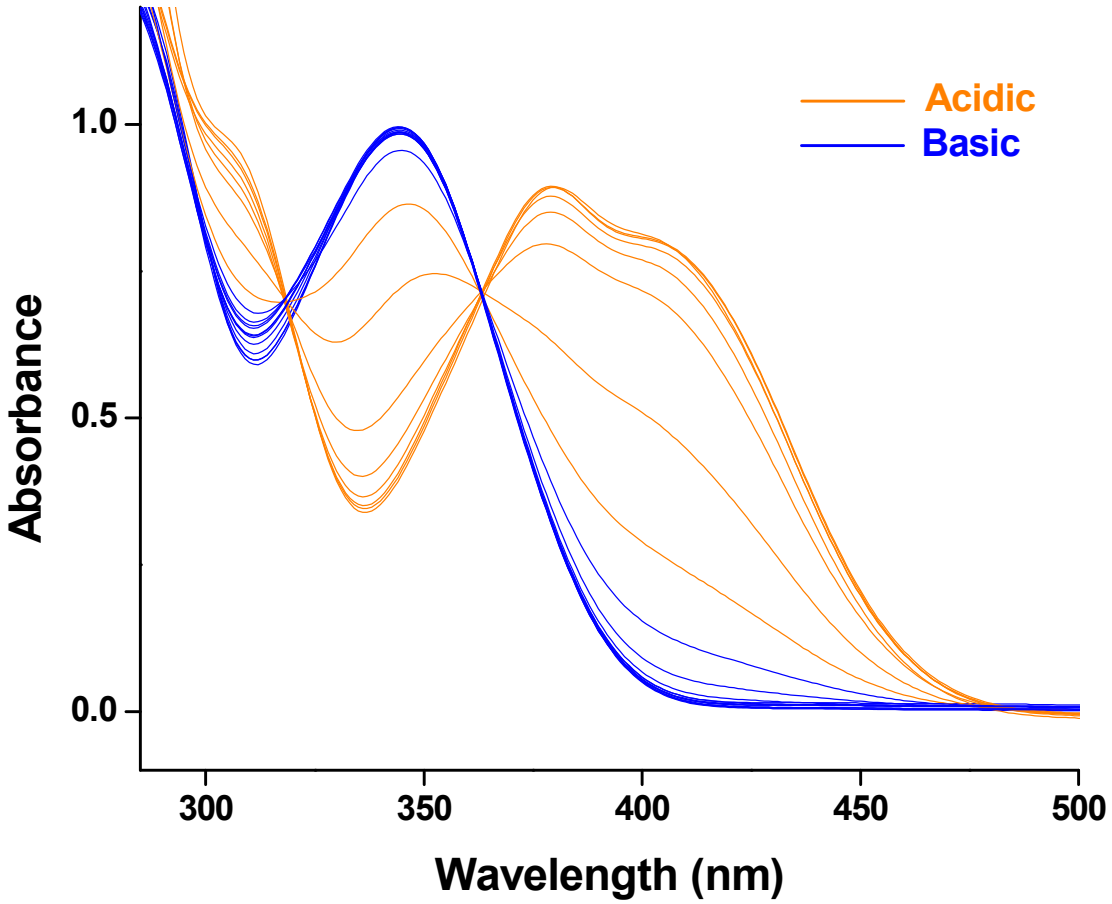

Fig. 4

RSC Advances Accepted Manuscript

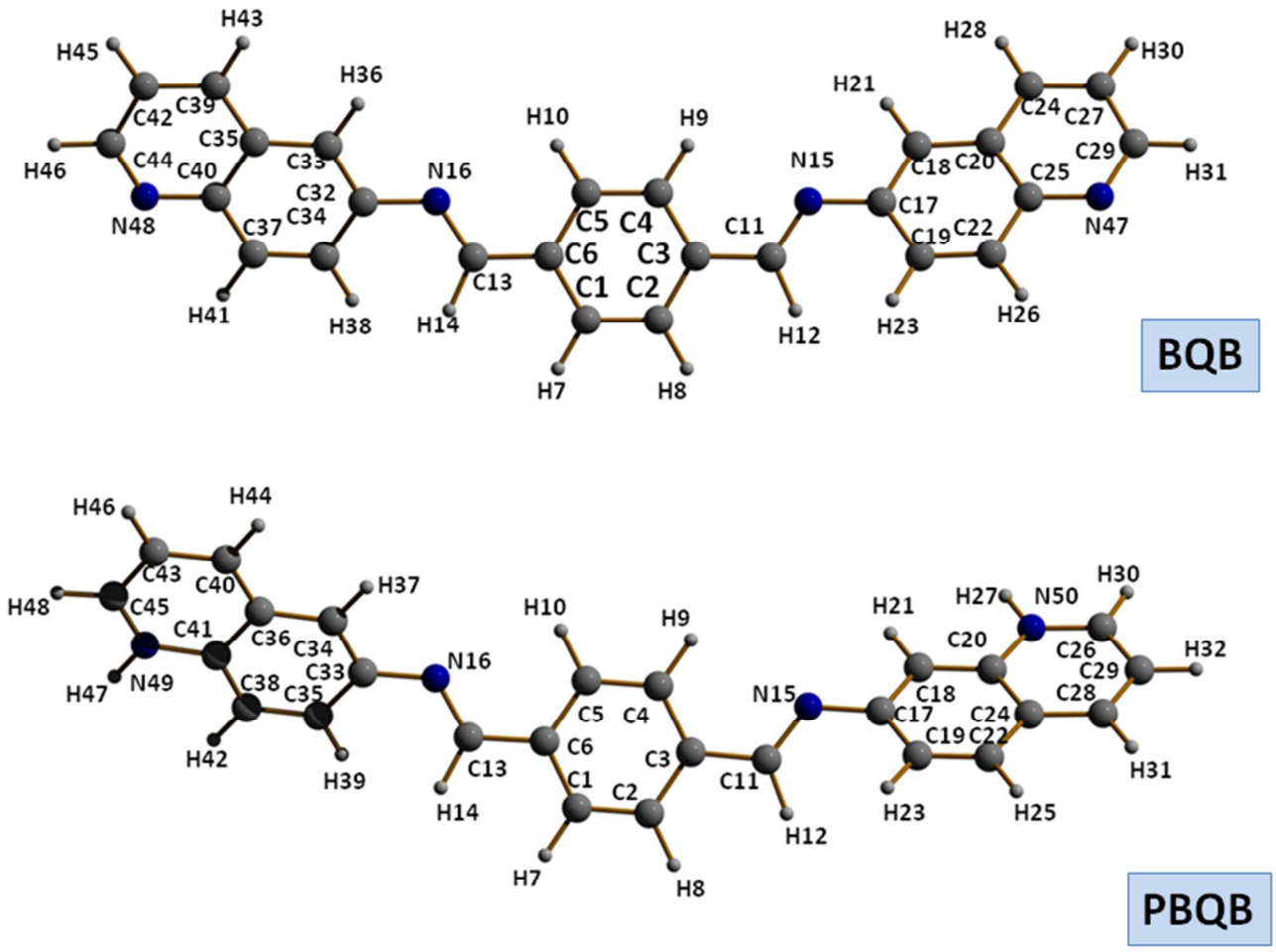

Fig. 5

RSC Advances Accepted Manuscript

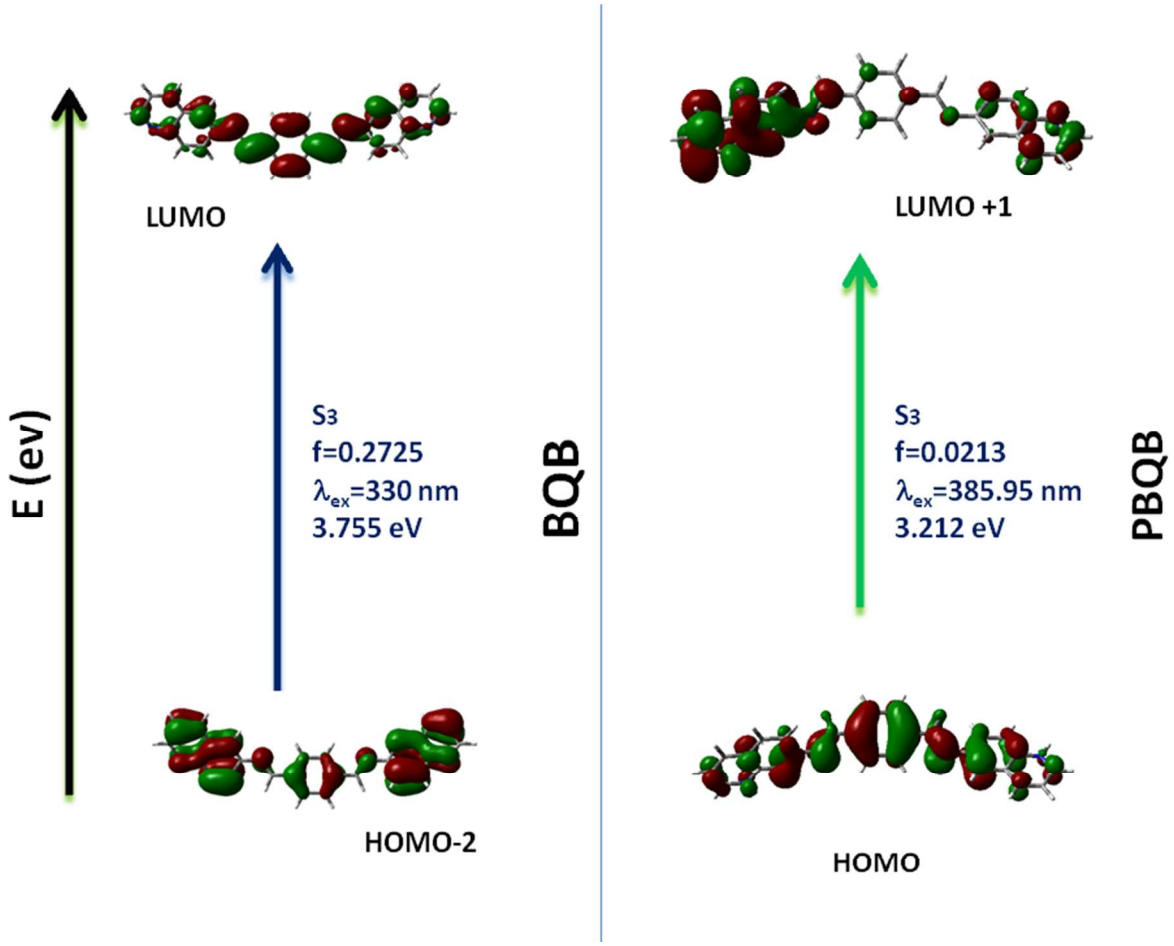

Fig. 6

RSC Advances Accepted Manuscript

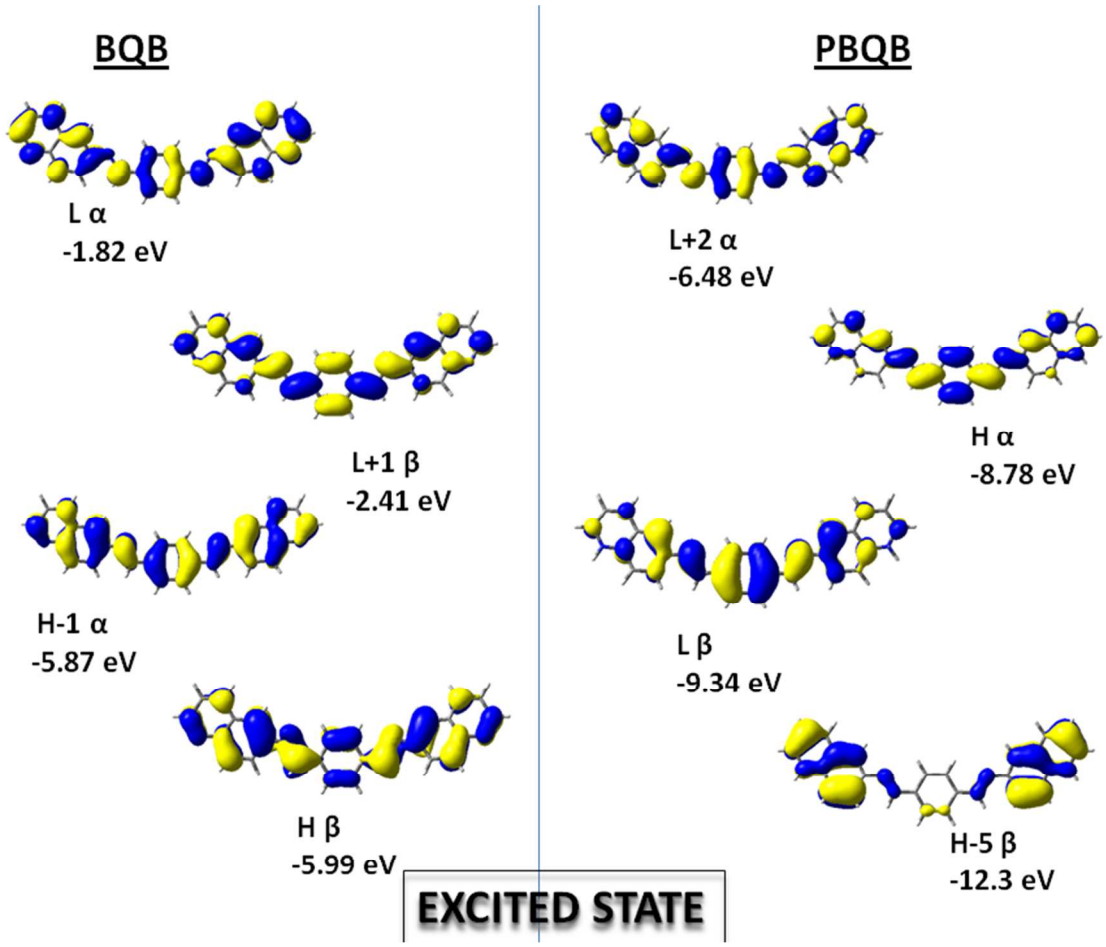

Fig. 7

RSC Advances Accepted Manuscript

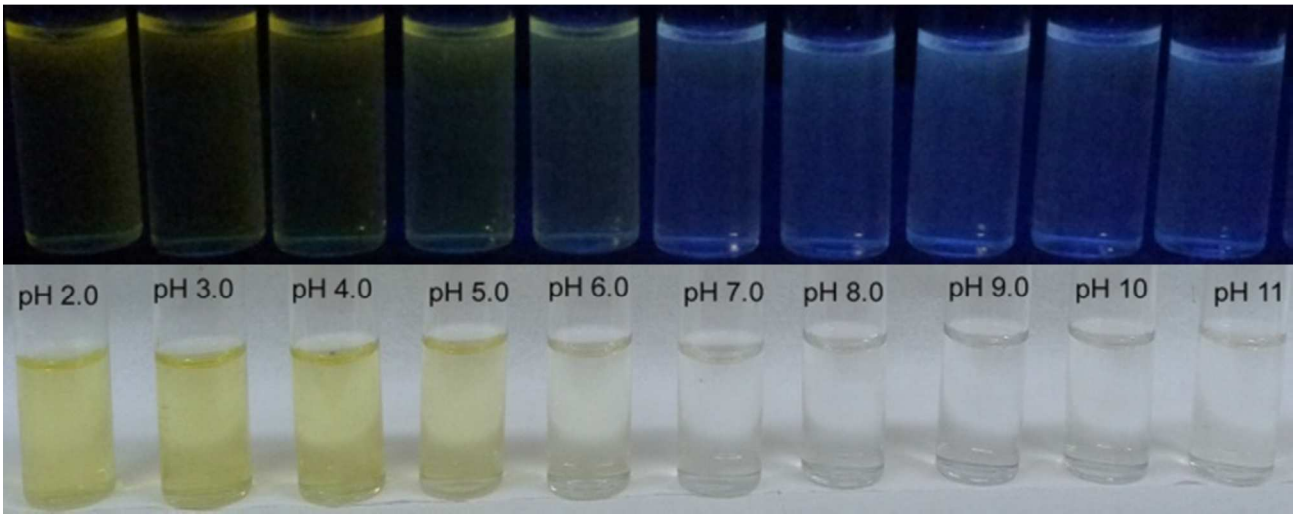

Fig. 8

RSC Advances Accepted Manuscript

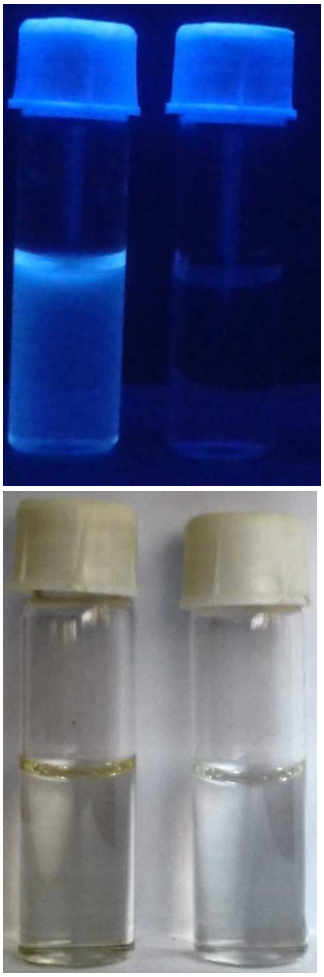

Fig. 9

RSC Advances Accepted Manuscript